Original Article

ORIGINAL ARTICLE

OLVERA ET AL.

LOW DOSE BP ENHANCES SCLAB-INDUCED TB MASS GAINS IN BRTL/+ OI MOUSE

Low Dose of Bisphosphonate Enhances Sclerostin Antibody-Induced Trabecular Bone Mass Gains in Brtl/+ Osteogenesis Imperfecta Mouse Model[1]

Diana Olvera,[1,2] Rachel Stolzenfeld,[1] Joan C Marini,[3] Michelle S Caird,[1] and Kenneth M Kozloff[1,2]

[1]Department of Orthopaedic Surgery, University of Michigan, Ann Arbor, MI, USA

[2]Department of Biomedical Engineering, University of Michigan, Ann Arbor, MI, USA

[3]Bone and Extracellular Matrix Branch, National Institute of Child Health and Human Disorders, National Institutes of Health, Bethesda, MD, USA

[1] This is the author manuscript accepted for publication and has undergone full peer review but has not been through the copyediting, typesetting, pagination and proofreading process, which may lead to differences between this version and the Version of Record. Please cite this article as doi:10.1002/jbmr.3421

ABSTRACT

Osteogenesis imperfecta (OI) is a genetic disorder characterized by altered bone quality and imbalanced bone remodeling, leading to skeletal fractures that are most prominent during childhood. Treatments for OI have focused on restoring pediatric bone density and architecture to recover functional strength and consequently reduce fragility. Though antiresorptive agents like bisphosphonates (BPs) are currently the most common intervention for the treatment of OI, a number of studies have shown efficacy of sclerostin antibody (SclAb) in inducing gains in bone mass and reducing fragility in OI mouse models. In this study, the effects of the concurrent use of BP and SclAb were evaluated during bone growth in a mouse harboring an OI-causing Gly→Cys mutation on col1a1. A single dose of antiresorptive BP facilitated the anabolic action of SclAb by increasing availability of surfaces for new bone formation via retention of primary trabeculae that would otherwise be remodeled. Chronic effects of concurrent administration of BP and SclAb revealed that accumulating cycles conferred synergistic gains in trabecular mass and vertebral stiffness, suggesting a distinct advantage of both therapies combined. Cortical gains in mass and strength occurred through SclAb alone, independent of presence of BP. In conclusion, these preclinical results support the scientific hypothesis that minimal antiresorptive treatment can amplify the effects of SclAb during early stages of skeletal growth to further improve bone structure and rigidity, a beneficial outcome for children with OI. © 2018 American Society for Bone and Mineral Research

KEY WORDS: OSTEOGENESIS IMPERFECTA; DISEASES AND DISORDERS OF/RELATED TO BONE; ANABOLICS; THERAPEUTICS, BONE QCT/MICROCT; ANALYSIS/QUANTITATION OF BONE; PRECLINICAL STUDIES; ANIMAL MODELS

Received in original form October 31, 2017; revised form February 27, 2018; accepted March 5, 2018. Accepted manuscript online March 15, 2018.

Address correspondence to: Kenneth Kozloff, PhD, Department of Orthopaedic Surgery, University of Michigan, Ann Arbor, MI , USA. E-mail: kenkoz@umich.edu

Additional Supporting Information may be found in the online version of this article.

Journal of Bone and Mineral Research, Vol. XX, No. X, Month 2018, pp XXXX–XXXX
DOI: 10.1002/jbmr.3421

Introduction

Osteogenesis imperfecta (OI) is a genetic bone disorder caused by collagen-related mutations resulting in type-dependent skeletal phenotypes ranging from subclinical to lethal severity.[1] Though these phenotypes are type-dependent, OI is most commonly associated with low bone mass, altered bone quality, and imbalanced bone remodeling leading to skeletal fractures and deformities such as scoliosis, short stature, and bowing of the long bones.[2] In the presence of OI, upregulation of osteoclast activity causes a cellular imbalance that favors resorption, resulting in thinner bones with fewer trabeculae, both of which greatly increase fracture risk during childhood.[3]

Despite no current cure for the disease, treatments for pediatric OI have focused on improving bone density to promote functional strength and consequently reduce bone fragility. Currently, antiresorptive agents from the class of bisphosphonates (BPs) are the standard of care for pediatric OI. Through their high affinity for calcium ions, these potent inhibitors of bone resorption strongly bind to hydroxyapatite bone surfaces where they can later be internalized by osteoclasts to interrupt the resorption process.[4] Several controlled clinical trials have established the beneficial effects of treating pediatric OI with BP, including decreased bone turnover and increased bone mineral density, particularly at sites of trabecular bone.[5–11] During endochondral growth, primary trabeculae are remodeled and converted to secondary spongiosa, and extended BP treatment interrupts this process, thus retaining calcified cartilage and increasing metaphyseal mass. In support of these studies, we and others have shown that with BP treatment, significant improvements in trabecular number, but not trabecular thickness are realized.[12–17] However, there remain concerns about the long-term treatment and retention of BPs in a growing skeleton,[18] and there remains a clinical need for additional therapeutic strategies that can minimize BP dose while maximizing therapeutic benefit.

Recently, sclerostin antibody (SclAb) has gained interest as an anabolic approach for the treatment of OI.[19–24] Sclerostin, expressed in mature osteocytes, inhibits bone

formation by exerting antagonistic effects on Wnt signaling and downstream osteoblast activity.[25] We have previously shown a significant anabolic response to SclAb in an OI mouse model.[19–23] These studies showed that treatment with a neutralizing antibody to sclerostin stimulated bone formation in cortical and trabecular bone, resulting in significant improvements in biomechanical properties. Unlike BPs, SclAb led to significant improvements in trabecular thickness. In the present study we sought to determine whether BPs could be used to augment SclAb efficacy by inducing retention of primary trabeculae, which could then serve as a substrate for the anabolic actions of SclAb to increase trabecular bone mass. We hypothesized that when combined, these two interventions would independently target different pathways of the bone remodeling cycle, leading to increases in trabecular bone mass greater than when either therapy was given alone. To accomplish this, in the present study, we test the immediate and long-term effects of treating rapidly growing Brtl/+ mice, harboring an OI-causing defect, with SclAb and BP together during growth. Our knock-in mouse model reproduces features of moderately severe Type IV OI. Treatment of Brtl/+ with alendronate alone increased trabecular bone mass through retention of calcified cartilage, with modest cortical gains that did not translate directly to biomechanical improvements.[17] Conversely, treatment of Brtl/+ with Scl-Ab alone elicited significant gains in both trabecular and cortical bone mass.[20] In the present study, through combination therapy, SclAb and BP induce gains in both trabecular thickness and number, leading to synergistic gains in trabecular bone stiffness, suggesting a distinct advantage to combination therapy in a growing mouse model of OI.

Materials and Methods

Animals

Wild-type (WT) and Brtl/+ mice with a mixed background of SV129/CD-1/C57BL/6S were derived from heterozygous Brtl/+ and WT parental strains.[26] To assess the short-term effects of pamidronate (PAM) and SclAb combined, at 21 days of age, male WT and Brtl/+ mice received a single intraperitoneal injection of PAM at either 0.3 mg/kg or 0.625 mg/kg (Sigma-Aldrich, St. Louis, MO, USA) or saline control. These doses of PAM represent 10% and 20% of doses shown to induce trabecular retention for 20 days in mice of similar age.[13] After a 3-day latency period, mice were randomly assigned to

SclAb treatment (Scl-Ab VI, 25 mg/kg; Amgen, Thousand Oaks, CA, USA) or saline groups and injected subcutaneously twice a week for 2 weeks (through day 34). SclAb was chosen at a dose that consistently induced an anabolic effect in our prior studies.[19–23] Calcein and alizarin were administered 1 day before PAM and at day 35, respectively, by intraperitoneal injection (30 mg/kg; Sigma-Aldrich, St. Louis, MO, USA) to visualize the growth pattern during treatment. Short-term treatment mice (n = 7/group) were euthanized at day 37. Similarly, to evaluate the long-term effects of PAM and SclAb combined, male WT and Brtl/+ mice received two cycles of combination therapy, repeating the treatment described above on day 38. Calcein, alizarin, and calcein were administered 1 day before cycle 1, 1 day before cycle 2, and at day 53, respectively, by intraperitoneal injection (30 mg/kg). Mice (n = 10/group) were euthanized at day 55. A summary of the experimental design for short-term and long-term assessment of combination therapy is shown in Fig. 1. All protocols and procedures were approved by the University of Michigan's Committee on Use and Care of Animals.

<Insert Figure 1>

Micro–computed tomography

To determine the short and long-term effects of PAM and SclAb on trabecular and cortical bone morphology, L_5 vertebrae and left femurs were scanned in water via micro–computed tomography (μCT) (eXplore Locus SP; GE Healthcare Pre-Clinical Imaging, London, ON, Canada). Scans were performed with the source set at 80 kVp and 80 μA using the Parker method of rotation (180 degrees plus a 20-degree fan angle), 0.5-degree increment angle, four frames averaged, and an acrylic beam flattener with a 0.02 Al filter were used for filtration of beam hardening artifacts. Images were reconstructed at a voxel size of 18 μm, and a hydroxyapatite-mimicking phantom was used to calibrate grayscale values for densitometry.[27]

Treatment of the growing skeleton with antiresorptive agents induces formation of a BP-laden band reflecting retention of primary spongiosa in the femur.[28,29] To study the short-term combined influence of PAM and SclAb on the femur, a 0.7-mm ROI was placed at this BP-induced retention region of the distal femur. A second ROI was located distal to the band (closer to the growth plate), representing bone formed subsequent to BP injection, during SclAb treatment. A third ROI was located proximal to the band

representing a site of trabecular bone formed prior to BP injection, but still under the influence of SclAb. A summary of the position of these ROIs are shown in Fig. 1*C*. Segmentation and binarization of trabecular bone at these sites was performed using a local threshold adjusted at each site for optimal representation of trabecular microarchitecture. Trabecular bone at and distal to BP band was segmented at 1500 Hounsfield units (HU), while trabecular bone found at the region proximal to BP band was segmented at 1300 HU.

To understand the resulting effects from concurrent cycles of combination therapy in the femur, a 4.5-mm ROI was placed at the metaphysis just proximal to the growth plate and extending through to the location of the proximal-most band of retained trabecular bone. To isolate the effects of each administered cyclic treatment, this full cycle ROI was broken down into representative regions of cycle 1 (2.7 mm) and cycle 2 (1.8 mm). Cycle 1 spanned from above the first BP band to right above the second induced BP band. Cycle 2 spanned above the second sclerotic BP band to right above the growth plate. A schematic of the placement of these three ROIs is shown in Fig. 1*D*. Due to the maturity of the bone and size of ROIs, a local auto-threshold was used to quantify trabecular bone at these three regions.[30]

Although a retention-related band was observed in the femur following BP treatment, a "bone in bone" appearance was induced in the vertebral body, consistent with vertebral growth patterns and clinical observations.[31] As a result, an ROI was placed between the cranial and caudal endplates of the L_5 vertebrae to analyze both short-term and long-term effects of combination treatment. Vertebral cortical and trabecular bone were separated through manual contouring to denote the outer and inner boundaries of the cortex and segmented by a local auto-threshold.

To measure both short-term and long-term effects of treatment on femoral cortical bone, an ROI spanning 15% of total femoral length was centered midway between the lateral third trochanter and the distal femoral growth plate in all samples. A local auto-threshold was used to quantify cortical bone. Bone architecture parameters (trabecular number [Tb.N], trabecular thickness [Tb.Th], bone volume fraction [BV/TV], and cortical thickness [C.Th]) were analyzed using commercially available software (MicroView Advanced Bone Analysis Application; GE Healthcare Pre-Clinical Imaging,

London, ON, Canada).

Bone histomorphometry

To qualitatively analyze bone formation response from short-term and long-term combination therapy, femurs and L_2 vertebrae were embedded without decalcification in methyl methacrylate. Both tissues were sectioned longitudinally with a Reichert-Jung Polycut microtome (Reichert-Jung, Germany) at a thickness of 8 μm and mounted on gelatin-coated glass slides. An upright microscope (Nikon Eclipse Ni-U) associated with a DS-Fi2 digital camera and NIS BR software (Nikon France, Champigny-sur-Marne, France) was used to acquire calcein and alizarin fluorescent images with a 10× dry objective.

Biomechanical testing

To assess the mechanical effects of short-term and long-term combination therapy, L_5 vertebrae (short-term and long-term) and left femurs (long-term only) were loaded to failure in compression and four-point bending, respectively, using an MTS 858 Mini-Bionix servo-hydraulic testing system (MTS Systems Corp., Eden Prairie, MN, USA). All specimens were kept hydrated in lactated Ringer's solution (LRS) prior to mechanical testing. The vertebral body was vertically aligned along its loading axis with an alignment pin (attached to lower platen and extending through the spinal column) and compressed to failure at a displacement rate of 0.05 mm/s. For four-point bending, the posterior surface of the femur was oriented in tension and the mid-diaphysis was loaded to failure at a displacement rate of 0.5 mm/s. Force and vertical displacements were continuously recorded throughout each test by a 50-lb load cell (Sensotec, Columbus, OH, USA) and an external linear variable differential transducer (LVDT; Lucas Schavitts, Hampton, VA, USA), respectively. A custom-developed LABVIEW program was used to calculate the mechanical properties for both tissues.

Statistics

Regional variations in bone architecture and biomechanics among the different treatments were determined using two-way ANOVA (GraphPad Prism 6.0; GraphPad Software, Inc., La Jolla, CA, USA) for each genotype independently. Values of $p < 0.05$ were considered significant, and significance is expressed on each plot for independent effects of PAM (vertical arrow) and SclAb (horizontal arrow) within each genotype. Data are

reported through dumbbell dot plots that display group means of PAM treatment (white markers) and PAM + SclAb treatment (solid markers) for both Brtl/+ (blue and circles) and WT (black and squares). Standard deviations are shown as shadows behind each marker.

Results

PAM and SclAb contribute distinct gains in distal femoral trabecular number and thickness following a single cycle of combination therapy

At the metaphyseal band site, where BP induces the greatest trabecular retention, PAM monotherapy induced a significant dose-dependent preservation of Tb.N at 0.3 mg/kg (Brtl/+ 3.297 ± 1.796/mm; WT 5.677 ± 1.446/mm) and 0.625 mg/kg (Brtl/+ 4.648 ± 1.471/mm; WT 6.225 ± 1.675/mm) compared to vehicle-treated control (Brtl/+ 1.905 ± 0.746/mm; WT 3.343 ± 0.574/mm; Fig. 2, Supporting Table 1). Although PAM solely acted to stabilize Tb.N, SclAb monotherapy induced significant gains in both Tb.Th (Brtl/+ 0.049 ± 0.004 mm; WT 0.059 ± 0.007 mm) and Tb.N (Brtl/+ 3.143 ± 0.574 mm; WT 5.272 ± 1.349 mm) compared to untreated control (Brtl/+ 0.035 ± 0.005 mm, 1.905 ± 0.746/mm; WT 0.037 ± 0.003 mm, 3.343 ± 0.574/mm). When PAM and SclAb were administered together, PAM continued to show no effect on Tb.Th, while SclAb triggered consistent thickness gains of 0.049 ± 0.008 mm for Brtl/+ and 0.067 ± 0.013 mm for WT across PAM doses. Interestingly, SclAb alone induced retention of Tb.N comparable to that of 0.3 mg/kg PAM alone (3.143 ± 1.133/mm versus 3.297 ± 1.796/mm). Together, combining SclAb and PAM during a single cycle of combination therapy contributed to a maximum increase in bone volume fraction of 0.263 ± 0.069 for Brtl/+ and 0.443 ± 0.130 for WT over untreated control (Brtl/+ 0.065 ± 0.027; WT 0.124 ± 0.025). Comparing regions proximal and distal to metaphyseal band, we noted that these effects were isolated to the site of concurrent drug administration (see Supporting Fig. 1). Trabecular bone distal to BP site showed minimal effect of BP as Tb.N was not significantly different from placebo. However, SclAb induced consistent gains in Tb.Th and Tb.N as monotherapy. At the proximal-most sites formed prior to BP intervention, BP effect was less evident, while significant gains in Tb.Th and BV/TV were still observed with SclAb.

<Insert Figure 2>

Multiple cycles helps stabilize bone mass gains from combination treatment

Following two cycles of combination therapy (Fig. 3*A*, Supporting Table 2), in trabecular regions extending across the entire metaphysis, PAM continued to show no effect on Tb.Th, acting solely to further stabilize Tb.N at 0.3 mg/kg (Brtl/+ 3.813 ± 0.856/mm; WT 4.557 ± 0.624/mm) and 0.625 mg/kg (Brtl/+ 4.329 ± 0.863/mm; WT 5.128 ± 0.687/mm) compared to untreated controls (Brtl/+ 2.929 ± 0.753/mm; WT 4.318 ± 1.131/mm). SclAb continued to induce gains in Tb.Th (Brtl/+ 0.050 ± 0.004 mm; WT 0.057 ± 0.006 mm), as well as a significant preservation of Tb.N (Brtl/+ 4.899 ± 0.595/mm; WT 5.796 ± 0.823/mm) across all PAM doses. As a result of these effects, maximum gains in bone volume fraction of 0.262 ± 0.057 for Brtl/+ and 0.362 ± 0.071 for WT were observed due to cumulative effects from both drugs compared to untreated control (Brtl/+ 0.107 ± 0.039; WT 0.189 ± 0.067). To further explore the effect of dose and time, the entire metaphyseal trabecular bone ROI was subdivided into two separate proximal and distal regions. The proximal-most region represented cycle 1 (Fig. 3*B*, Supporting Table 2), and represents the fate of the band explored in Fig. 2 following a second cycle of therapy. During a typical course of therapy, BP will interfere with the growth-associated trabecular modeling that would normally cause trabeculae to gradually disappear during growth, thus stabilizing trabecular number over time. Here (Fig. 3*B*, Supporting Table 2), Tb.N of PAM-alone animals drops below levels shown in Fig. 2, confirming that the low dose of PAM was insufficient to stabilize bone mass long-term. Although the low dose of PAM was sufficient to restore Brtl/+ Tb.N to WT levels after the first cycle, the higher dose was required for the rescue effects to sustain throughout the second cycle. The distal-most region chosen represented cycle 2 (Fig. 3*C*, Supporting Table 2), and shows the retention band induced by the second PAM administration in the presence or absence of SclAb. Here, progressive gains in Tb.N are apparent, and Tb.Th gains in response to SclAb following cycle 2 (Brtl/+ 29%: WT 28%) were substantially less than those observed in the proximal region of interest (Brtl/+ 53%; WT 53%), reflecting either the shorter treatment duration for this site, or a saturation effect of SclAb on trabecular thickness.

<Insert Figure 3>

Multiple treatments of PAM and SclAb significantly slows the turnover of primary

spongiosa

To assess the fate of bone formed during a single treatment cycle (Fig. 4*A*), calcein (green) was administered at the beginning of PAM (or control) and alizarin (red) at the end of SclAb (or control) treatment. Using this labeling scheme, bone formed and retained following PAM is shown in green, while bone formed subsequent to PAM is green. During growth, untreated Brtl/+ control showed a significant loss of primary trabeculae, reflected by total absence of green trabecular label (Fig. 4*A*, top left). PAM alone increased preservation of trabecular bone shown by retained spicules of calcein label (Fig. 4*A*, top right). In contrast SclAb alone (Fig. 4*A*, bottom left) exhibited retention of calcein label with adjacent alizarin-labeled bone, indicating trabecular thickening on preserved primary spongiosa. Combined, SclAb and PAM induced an additive bone mass response at the site of concurrent drug administration (Fig. 4*A*, bottom right). These patterns of trabecular preservation and thickening amplify under the influence of two cycles of therapy (Fig. 4*B*) as gains expand further down the proximal femur compared to gains seen after one cycle (Fig. 4*A*). Significant preservation of second-cycle Tb.N is apparent from alizarin-labeled trabeculae in PAM-treated femurs (Fig. 4*B*, top right), whereas SclAb alone led to both retention of trabeculae and thickening, indicated by alizarin-labeled trabeculae with abundant calcein label (Fig. 4*B*, bottom left). Robust gains in trabeculae and thickness are appreciated when both drugs were given together in multiple cycles as seen through retained alizarin-labeled trabeculae with a calcein-labeled thickness (Fig. 4*B*, bottom right).

<Insert Figure 4>

Multiple cycles of combination therapy induce synergistic gains in vertebral trabecular bone mass

Microstructural analysis of the lumbar vertebra demonstrated similar findings, albeit to a lesser extent, as seen in the femoral metaphysis, confirming consistency of effects at axial and appendicular sites. Under the influence of a single treatment cycle (Fig. 5*A*, Supporting Table 3), PAM monotherapy significantly stabilized Tb.N at 0.3 mg/kg (Brtl/+ 6.137 ± 0.536/mm; WT 6.573 ± 0.459/mm) and 0.625 mg/kg (Brtl/+ 6.376 ± 0.569/mm; WT 6.886 ± 0.363/mm) over placebo control (Brtl/+ 5.787 ± 0.300/mm; WT 6.130 ± 0.271/mm), with no effect on Tb.Th. SclAb monotherapy produced gains in both

Tb.N (Brtl/+ 6.208 ± 0.420/mm; WT 6.816 ± 0.376/mm) and Tb.Th (Brtl/+ 0.046 ± 0.002 mm; WT 0.053 ± 0.004 mm). As found in the femur, when SclAb was administered with PAM, little additional gains were observed in Tb.N. Higher doses of PAM were required to see additional trabecular thickening in Brtl/+, while WT showed an average 0.055 mm increase in Tb.Th with the two drugs combined. Despite these observations during a single cycle of combination therapy, overall gains in BV/TV were comparable whether drugs were given combined (Brtl/+ 0.298 0.043; WT 0.388 ± 0.029) or SclAb alone (Brtl/+ 0.289 ± 0.032; WT 0.365 ± 0.040). Lumbar vertebrae benefited strongly from two treatment cycles (Fig. 5*B*), triggering a maximum synergistic response on BV/TV (Brtl/+ 0.421 ± 0.053; WT 0.504 ± 0.053) over placebo (Brtl/+ 0.235 ± 0.026; WT 0.293 ± 0.037) compared to 0.625 mg/kg PAM (Brtl/+ 0.275 ± 0.046; WT 0.315 ± 0.033) and SclAb (Brtl/+ 0.339 ± 0.043; WT 0.452 ± 0.065) monotherapy. PAM continued to increase bone mass through Tb.N at 0.3 mg/kg (Brtl/+ 6.002 ± 0.444/mm; WT 6.487 ± 0.346/mm) and at 0.625 mg/kg (Brtl/+ 6.300 ± 0.614/mm; WT 6.838 ± 0.340/mm) with no effect on Tb.Th. SclAb induced strong gains in both Tb.N (Brtl/+ 6.867/mm; WT 6.889/mm) and Tb.Th (Brtl/+ 0.058 ± 0.004mm; WT 0.070 ± 0.007 mm) across all PAM dosages, contributing substantially to the overall synergistic gains in lumbar vertebrae trabecular bone mass.

<Insert Figure 5>

Substantial preservation of Tb.N and increased Tb.Th in vertebral body

To evaluate the response of newly formed bone under the effects of a single treatment cycle (Fig. 6*A*), calcein (green) was administered prior to PAM treatment and alizarin (red) after SclAb treatment. Brtl/+ control showed few primary trabeculae labeled with calcein, which was stabilized with a single dose of PAM. SclAb showed preservation of calcein labeled bone with alizarin labeled perimeters suggesting trabecular thickening. These observations confirm the antiresorptive and anabolic effects of both treatments, which led to further additive gains in bone mass. Newly formed bone under the effects of multiple treatment cycles (Fig. 6*B*), was labeled with calcein (green) at the beginning of treatment, alizarin (red) between cyclic treatments and again with calcein (green) at the end of treatment. Labeling of control samples showed considerable loss of primary trabeculae. PAM alone promoted the retention of primary trabeculae, noted by

considerable alizarin-labeled bone adjacent to the growth plates. SclAb alone triggered both trabecular retention and thickness gains. Combination of both drugs administered cyclically induced a robust trabecular response which extended to the periosteal bone surface.

<Insert Figure 6>

PAM intervention does not interfere with SclAb ability to improve femoral rigidity

PAM effects were isolated to the lumbar vertebrae and femoral trabecular bone, with no apparent effects on femoral diaphyseal cortical bone structure or biomechanical properties. Rather, gains in cortical thickness were solely attributed to SclAb because our administered PAM treatment used doses significantly lower than those used in human studies. After a single cycle of combination therapy (Fig. 7*A*, Supporting Table 4), SclAb monotherapy induced greater gains in femoral C.Th (Brtl/+ 0.182 ± 0.008 mm; WT 0.234 ± 0.009 mm) than when combined with 0.3 mg/kg PAM (Brtl/+ 0.171 ± 0.017 mm; WT 0.234 ± 0.009 mm) or 0.625 mg/kg PAM (Brtl/+ 0.176 ± 0.012 mm; WT 0.216 ± 0.028 mm) compared to placebo (Brtl/+ 0.152 ± 0.016 mm; WT 0.192 ± 0.022 mm). However, this effect was transient, because after two cycles (Fig. 7*B*), consistent C.Th gains of 0.231 ± 0.023 mm in Brtl/+ and 0.277 ± 0.023 mm in WT were observed across all PAM doses. As a result of these C.Th changes, SclAb consistently improved femoral rigidity through gains in stiffness (Brtl/+ 231.768 ± 44.278 N/mm; WT 272.632 ± 57.425 N/mm) and ultimate load (Brtl/+ 35.379 ± 6.741 N; WT 47.816 ± 9.937 N) across all PAM doses, driven by gains in bending moment (Brtl/+ 0.158 ± 0.045 mm^4; WT 0.207 ± 0.028 mm^4) and cross-sectional area (Brtl/+ 1.919 ± 0.200 mm^2; WT 2.234 ± 0.267 mm^2).

<Insert Figure 7>

PAM and SclAb synergistically improve Brtl/+ vertebral stiffness over monotherapy effects

Similar to the cortical effects seen in the femur, C.Th gains in the vertebral body were influenced by SclAb, not PAM. A single cycle of combination therapy (Fig. 8*A*, Supporting Table 5) resulted in lower gains in C.Th at 0.3 mg/kg (Brtl/+ 0.086 ± 0.007 mm; WT 0.102 ± 0.006 mm) and 0.625 mg/kg (Brtl/+ 0.088 ± 0.007 mm; WT 0.102 ± 0.007 mm) than SclAb monotherapy (Brtl/+ 0.091 ± 0.005mm; WT 0.100 ± 0.005 mm). However, with multiple cycles (Fig. 8*B*), greater gains in C.Th were achieved at 0.3

mg/kg (Brtl/+ 0.090 ± 0.006 mm; WT 0.103 ± 0.010 mm) and 0.625 mg/kg (Brtl/+ 0.093 ± 0.009 mm; WT 0.106 ± 0.008 mm). Functionally, over a single cycle of therapy (Fig. 8*C*), PAM dose-dependently improved vertebral stiffness and SclAb amplified this response (Brtl/+ 29%, WT 32%). Improvements in ultimate load were attributed to SclAb with gains of 48% in Brtl/+ and 58% in WT. Over two cycles of combination treatment (Fig. 8*D*), maximum gains in vertebral stiffness were observed when both PAM (Brtl/+ 75.650 ± 8.031 N/mm; WT 119.729 ± 24.514 N/mm) and SclAb (Brtl/+ 81.307 ± 15.531 N/mm; WT 136.688 ± 16.367 N/mm) were administered alone. When administered together in sequential cycles, WT showed maximum additive gains (156.340 ± 28.962 N/mm) compared to each treatment alone. Remarkably, a synergistic response was observed in Brtl/+, with a maximum stiffness increase of 130.945 ± 25.920 N/mm compared to placebo control (46.974 ± 20.181 N/mm).

<Insert Figure 8>

Discussion

The results in this study show Brtl–IV mice with a genetic knock-in for moderately severe Type IV OI responded favorably to repeated cycles of a single dose of antiresorptive PAM in combination with anabolic SclAb. The immediate effects of this combination therapy showed that both interventions stimulated gains in bone mass through different means, leading to overall improvements in biomechanical function. Although a preservation of Tb.N was observed through PAM, SclAb led to gains in both Tb.N and Tb.Th, as well as a significant cortical bone response. When this combination therapy was administered twice cyclically, the resulting gains in trabecular bone mass were dependent on anatomic site; cumulative for long bones and synergistic for the vertebral body. These findings may have a strong clinical utility to increase bone mass in OI patients—particularly those with excessive high bone turnover leading to severe trabecular osteopenia that might make them more resistant to anabolic therapy alone.

Antiresorptive BPs continue to be the most common intervention used in pediatric OI. Numerous studies have shown a favorable bone response to BP therapy in both preclinical studies using OI mouse models[12,17,32,33] and clinical studies of children with OI.[7,9,33–37] By their antiresorptive activity, BPs have been proposed to decrease the high bone turnover characteristic of OI, increase metaphyseal bone mass by increasing

trabecular number, and increase cortical bone mass by inhibiting endosteal resorption. However, concern for long half-life,[38] microdamage accumulation,[39] and delayed healing[40] have led to attempts to minimize treatment dose.[18] Recently, SclAb has gained interest as a promising anabolic approach for the treatment of OI. In contrast to BP, SclAb has been shown to increase trabecular bone mass in OI models through trabecular thickening, and increase cortical bone mass through periosteal apposition.[19,20,22] Furthermore, in a growing model, periosteal apposition will occur as a result of growth, which contributes to further bone mass gains because PAM has not been shown to affect non-remodeling surfaces. Therefore, we hypothesized that a combination of these two agents may lead to additive if not synergistic structural and functional gains. When given together, we observed that BPs induce retention of primary trabeculae, which can serve as a substrate for the subsequent anabolic response of SclAb, whereas cortical bone mass gains resulted from SclAb alone.

Combination effects have been explored with BP following SclAb in order to preserve gains in bone mass following cessation of drug clinically[41] and in OI models.[23] Alternatively, SclAb following BP has been explored using ovariectomized rats in which SclAb induced gains in bone mass regardless of prior BP exposure.[42] This study was performed in aged, osteoporotic rats, which have considerably different growth plate dynamics than in the present study. In another OI mouse model, SclAb was combined with zoledronic acid,[43] where no synergistic effects were observed. Rather, the treatment effect from zoledronic acid alone led to >300% gains in proximal tibial trabecular bone volume fraction, with no additional gains observed when zoledronic acid was combined with SclAb. In the present combination study, we likely avoided this saturation response with lower doses of BP, triggering more modest trabecular preservation, allowing SclAb to synergistically increase bone mass by increasing trabecular thickness.

The present study differs from these other combination therapy studies because we aimed to explore low doses of PAM which, if given alone, would be insufficient to generate long-term preservation of trabecular bone. Indeed, when tracking the fate of the trabecular bone generated by the first cycle of PAM, we observed a lack of long-term antiresorptive effects, particularly in the vertebrae. Yet when administered together with

SclAb, both drugs combined led to cumulative gains on bone mass. At the site of concurrent treatment, PAM induced a sclerotic metaphyseal band consistent with previous observations of BP treatment stabilizing primary spongiosa near the growth plate.[44] Treatment with PAM alone showed a significant effect on bone volume fraction for both Brtl/+ and WT when compared to untreated controls, solely due to a significant dose-dependent preservation of Tb.N with no concurrent effect on Tb.Th. Similar gains in bone volume were triggered with SclAb monotherapy; however, these were attributed to an effect on both Tb.N and Tb.Th. Gains in Tb.Th likely resulted from a direct anabolic effect on existing trabecular bone. However, gains in Tb.N could have resulted from either stabilization of thin trabeculae destined for remodeling via increased bone formation on those surfaces, or through a mild antiresorptive effect, because SclAb has been shown to have both anabolic and anticatabolic actions.[45] Indeed, SclAb alone preserved Tb.N to levels equivalent to low-dose PAM, suggesting a similar potency of antiresorptive action between the two drugs. When given together, extended gains in trabecular bone mass were attributed to SclAb-induced trabecular thickening at sites formed following PAM exposure and retention of trabecular number. These observations were confirmed through histomorphometry. Observations at sites distal and proximal to the metaphyseal band helped verify that PAM bone response was constrained to its induced sclerotic band, while SclAb led to trabecular thickening away from these sites.

The same trabecular response was observed in the vertebral body for both Brtl/+ and WT, to a slightly greater extent, as was observed in the femoral metaphysis. These findings are consistent with other BP studies that show a variable BP binding and bone density response between axial versus appendicular, and cortical versus trabecular sites.[29,46] Following two cycles of combination therapy, a synergistic effect on bone mass was observed in the vertebral body that was not observed in the femoral metaphysis, which instead showed an additive effect of the two interventions. Histomorphometry of two cycles of combination therapy demonstrated thickened bands of retained primary spongiosa emerging from both growth plates of the vertebra consistent observations in other pediatric BP studies.[31,47,48]

In addition to trabecular effects, SclAb induced an anabolic response in femoral and vertebral cortical bone, because gains observed were solely attributed to SclAb, even

when administered in combination with PAM. This increase in cortical thickness correlates with previous findings where growing Brtl/+ mice treated with SclAb showed cortical thickness gains in the femoral midshaft over a similar treatment duration.[20] Furthermore, progressive gains in cortical thickness were observed comparing one versus two cycles of SclAb monotherapy. Although clinical studies of children with OI have shown slight changes in cortical bone from PAM treatment,[17,49–51] in the present study, PAM had no effect on cortical thickness, likely due to the low treatment duration and doses used in the present study compared to those in clinical trials. Low doses of PAM were deliberately chosen for this study in order to minimize the antiresorptive effect and not mask the potential combination effects hypothesized from both drugs together.

Two cycles of PAM monotherapy showed no effect on femoral stiffness or load in either Brtl/+ and WT. SclAb, on the other hand, improved both stiffness and load as a result of the strong anabolic effect on cortical bone. When both drugs were administered concurrently, SclAb continued to be the sole contributor to these improvements in whole-bone mechanical properties.

Similarly, in the vertebral body, Brtl/+ ultimate load was only improved by SclAb, yet both PAM and SclAb led to strong gains in vertebral stiffness. In fact, following two cycles of combined treatment, Brtl/+ stiffness improved synergistically when compared to combined effects from monotherapy of either drug. This finding may have important implications for treatment of spinal deformities in OI. Deformation of the spine arises from both anatomical and functional factors resulting from the OI phenotype. Depending on the severity of the deformity or fracture frequency, prophylactic interventions like BP treatment can potentially reduce fracture incidence. Combining SclAb with PAM stabilized vertebral trabecular bone resulting in significant gains in vertebral stiffness. SclAb alone improved maximum load, likely due to additional gains in cortical thickness that were not evident following PAM. These findings confirm other studies that have shown that C.Th is a primary determinant feature for compressive strength of the whole vertebral body.[52–54]

This study has several limitations. Because OI is a disease of many mutations, the results of this study may not extend to all types of OI. Additionally, the Brtl/+ mouse fragility phenotype is of moderate severity, and the mouse does not suffer spontaneous

fractures. In addition, the study was only performed in male mice and it is now well established that gender can affect the outcome of drug treatments. Furthermore, BP action when given after closure of the growth plate during skeletal maturity will not yield the same findings as observed in this study because turnover of primary spongiosa will be nonexistent. In many of our outcomes, treatment with our lowest PAM dose alone improved bone mass to WT control levels, effectively rescuing the phenotype, while our higher PAM dose induced gains in bone mass greater than WT baseline. Although our goal was not to directly titrate our treatment outcomes to match untreated WT levels, we believe that further adjustment of treatment doses and/or duration will vary depending on clinical severity to best represent a "rescue" response.

SclAb has been proposed as a novel anabolic intervention to treat the low bone mass and fragility phenotype present in patients with OI. The results in this study extend our previous observations of single-drug therapy in Brtl/+[17,20] and show the benefits of combining SclAb with antiresorptive treatment during growth. In severe cases of OI, where extreme low bone mass may result from excessive resorption of primary trabeculae during endochondral growth, SclAb alone might not be enough to significantly improve trabecular bone volume because of lack of bone upon which to exert an anabolic action. Thus, in cases of extreme low bone mass, concurrent antiresorptive and anabolic therapy might further improve bone formation outcomes. Importantly, these results suggest that modest doses of BP, which would otherwise not induce a sustained therapeutic effect, may be sufficient to preserve trabecular architecture enough to permit an anabolic action of SclAb on bone which would otherwise be remodeled. Together, these preclinical results support the scientific premise that antiresorptive and anabolic combination therapy during early stages of skeletal growth can help induce greater gains in bone mass in OI than either drug alone. The present data provides key preclinical results to support a treatment plan to maximize combination therapy in OI, or other diseases associated with low bone mass during pediatric growth and development.

Disclosures

Acknowledgments

Financial support from NIH to KMK (R01AR062522) is gratefully acknowledged. Additional research support was received from NIH (P30AR069620). SclAb was

provided by Amgen and UCB Pharma. We thank Bonnie Nolan and Carol Whitinger for their contributions.

Authors' roles: Study designed and conducted by DO, RS, and KMK. Data collected by DO and RS. Data analyzed and interpreted by DO, RS, MSC, JCM, and KMK. Manuscript was written by DO and KMK and revised and approved by all authors. KMK takes responsibility for the integrity of the data analysis.

References

1. Forlino A, Marini JC. Osteogenesis imperfecta. Lancet. 2016;387(10028):1657–71.

2. Rauch F, Glorieux FH. Osteogenesis imperfecta. Lancet. 2004;363(9418):1377–85.

3. Roughley PJ, Rauch F, Glorieux FH. Osteogenesis imperfecta—clinical and molecular diversity. Eur Cell Mater. 2003;5:41–7; discussion 7.

4. Russell RG, Croucher PI, Rogers MJ. Bisphosphonates: pharmacology, mechanisms of action and clinical uses. Osteoporos Int. 1999;9 Suppl 2:S66–80.

5. Land C, Rauch F, Travers R, Glorieux FH. Osteogenesis imperfecta type VI in childhood and adolescence: effects of cyclical intravenous pamidronate treatment. Bone. 2007;40(3):638–44.

6. Castillo H, Samson-Fang L. Effects of bisphosphonates in children with osteogenesis imperfecta: an AACPDM systematic review. Dev Med Child Neurol. 2009;51(1):17–29.

7. Rauch F, Munns CF, Land C, Cheung M, Glorieux FH. Risedronate in the treatment of mild pediatric osteogenesis imperfecta: a randomized placebo-controlled study. J Bone Miner Res. 2009;24(7):1282–9.

8. Salehpour S, Tavakkoli S. Cyclic pamidronate therapy in children with osteogenesis imperfecta. J Pediatr Endocrinol Metab. 2010;23(1–2):73–80.

9. Bishop N, Harrison R, Ahmed F, et al. A randomized, controlled dose-ranging study of risedronate in children with moderate and severe osteogenesis imperfecta. J Bone Miner Res. 2010;25(1):32–40.

10. Bishop N, Adami S, Ahmed SF, et al. Risedronate in children with osteogenesis imperfecta: a randomised, double-blind, placebo-controlled trial. Lancet. 2013;382(9902):1424–32.

11. Palomo T, Andrade MC, Peters BS, et al. Evaluation of a modified pamidronate protocol for the treatment of osteogenesis imperfecta. Calcif Tissue Int. 2016;98(1):42–8.

12. Camacho NP, Raggio CL, Doty SB, et al. A controlled study of the effects of alendronate in a growing mouse model of osteogenesis imperfecta. Calcif Tissue Int. 2001;69(2):94–101.
13. Zhu ED, Louis L, Brooks DJ, Bouxsein ML, Demay MB. Effect of bisphosphonates on the rapidly growing male murine skeleton. Endocrinology. 2014;155(4):1188–96.
14. Evans KD, Sheppard LE, Rao SH, Martin RB, Oberbauer AM. Pamidronate alters the growth plate in the oim mouse model for osteogenesis imperfecta. Int J Biomed Sci. 2009;5(4):345–52.
15. Rao SH, Evans KD, Oberbauer AM, Martin RB. Bisphosphonate treatment in the oim mouse model alters bone modeling during growth. J Biomech. 2008;41(16):3371–6.
16. McCarthy EA, Raggio CL, Hossack MD, et al. Alendronate treatment for infants with osteogenesis imperfecta: demonstration of efficacy in a mouse model. Pediatr Res. 2002;52(5):660–70.
17. Uveges TE, Kozloff KM, Ty JM, et al. Alendronate treatment of the Brtl osteogenesis imperfecta mouse improves femoral geometry and load response before fracture but decreases predicted material properties and has detrimental effects on osteoblasts and bone formation. J Bone Miner Res. 2009;24(5):849–59.
18. Vasanwala RF, Sanghrajka A, Bishop NJ, Hogler W. Recurrent proximal femur fractures in a teenager with osteogenesis imperfecta on continuous bisphosphonate therapy: are we overtreating? J Bone Miner Res. 2016;31(7):1449–54.
19. Sinder BP, White LE, Salemi JD, et al. Adult Brtl/+ mouse model of osteogenesis imperfecta demonstrates anabolic response to sclerostin antibody treatment with increased bone mass and strength. Osteoporos Int. 2014;25(8):2097–107.
20. Sinder BP, Salemi JD, Ominsky MS, Caird MS, Marini JC, Kozloff KM. Rapidly growing Brtl/+ mouse model of osteogenesis imperfecta improves bone mass and strength with sclerostin antibody treatment. Bone. 2015;71:115–23.
21. Sinder BP, Lloyd WR, Salemi JD, et al. Effect of anti-sclerostin therapy and osteogenesis imperfecta on tissue-level properties in growing and adult mice while controlling for tissue age. Bone. 2016;84:222–9.
22. Sinder BP, Eddy MM, Ominsky MS, Caird MS, Marini JC, Kozloff KM. Sclerostin antibody improves skeletal parameters in a Brtl/+ mouse model of osteogenesis

imperfecta. J Bone Miner Res. 2013;28(1):73–80.
23. Perosky JE, Khoury BM, Jenks TN, et al. Single dose of bisphosphonate preserves gains in bone mass following cessation of sclerostin antibody in Brtl/+ osteogenesis imperfecta model. Bone. 2016;93:79–85.
24. Glorieux FH, Devogelaer JP, Durigova M, et al. BPS804 anti-sclerostin antibody in adults with moderate osteogenesis imperfecta: results of a randomized phase 2a trial. J Bone Miner Res. 2017;32(7):1496–504.
25. Poole KE, van Bezooijen RL, Loveridge N, et al. Sclerostin is a delayed secreted product of osteocytes that inhibits bone formation. FASEB J. 2005;19(13):1842–4.
26. Forlino A, Porter FD, Lee EJ, Westphal H, Marini JC. Use of the Cre/lox recombination system to develop a non-lethal knock-in murine model for osteogenesis imperfecta with an alpha1(I) G349C substitution. Variability in phenotype in BrtlIV mice. J Biol Chem. 1999;274(53):37923–31.
27. Meganck JA, Kozloff KM, Thornton MM, Broski SM, Goldstein SA. Beam hardening artifacts in micro-computed tomography scanning can be reduced by X-ray beam filtration and the resulting images can be used to accurately measure BMD. Bone. 2009;45(6):1104–16.
28. Glorieux FH, Bishop NJ, Plotkin H, Chabot G, Lanoue G, Travers R. Cyclic administration of pamidronate in children with severe osteogenesis imperfecta. N Engl J Med. 1998;339(14):947–52.
29. Kozloff KM, Volakis LI, Marini JC, Caird MS. Near-infrared fluorescent probe traces bisphosphonate delivery and retention in vivo. J Bone Miner Res. 2010;25(8):1748–58.
30. Otsu N. A threshold selection method from gray-level histograms. IEEE Trans Syst Man Cybern. 1979;9(1):62–6.
31. Chakraborty PP, Biswas SN, Patra S, Santra G. “Zebra stripe” sign and “bone in bone” sign in cyclical bisphosphonate therapy. J Clin Diagn Res. 2017;11(2):RJ01–2.
32. Boskey AL, Marino J, Spevak L, et al. Are changes in composition in response to treatment of a mouse model of osteogenesis imperfecta sex-dependent? Clin Orthop Relat Res. 2015;473(8):2587–98.
33. Hald JD, Evangelou E, Langdahl BL, Ralston SH. Bisphosphonates for the prevention of fractures in osteogenesis imperfecta: meta-analysis of placebo-controlled

trials. J Bone Miner Res. 2015;30(5):929–33.
34. Gatti D, Antoniazzi F, Prizzi R, et al. Intravenous neridronate in children with osteogenesis imperfecta: a randomized controlled study. J Bone Miner Res. 2005;20(5):758–63.
35. Letocha AD, Cintas HL, Troendle JF, et al. Controlled trial of pamidronate in children with types III and IV osteogenesis imperfecta confirms vertebral gains but not short-term functional improvement. J Bone Miner Res. 2005;20(6):977–86.
36. Sakkers R, Kok D, Engelbert R, et al. Skeletal effects and functional outcome with olpadronate in children with osteogenesis imperfecta: a 2-year randomised placebo-controlled study. Lancet. 2004;363(9419):1427–31.
37. Ward LM, Rauch F, Whyte MP, et al. Alendronate for the treatment of pediatric osteogenesis imperfecta: a randomized placebo-controlled study. J Clin Endocrinol Metab. 2011;96(2):355–64.
38. Papapoulos SE, Cremers SCLM. Prolonged bisphosphonate release after treatment in children. N Engl J Med. 2007;356(10):1075–6.
39. Komatsubara S, Mori S, Mashiba T, et al. Suppressed bone turnover by long-term bisphosphonate treatment accumulates microdamage but maintains intrinsic material properties in cortical bone of dog rib. J Bone Miner Res. 2004;19(6):999–1005.
40. Anam EA, Rauch F, Glorieux FH, Fassier F, Hamdy R. Osteotomy healing in children with osteogenesis imperfecta receiving bisphosphonate treatment. J Bone Miner Res. 2015;30(8):1362–8.
41. Recknor CP, Recker RR, Benson CT, et al. the effect of discontinuing treatment with blosozumab: follow-up results of a phase 2 randomized clinical trial in postmenopausal women with low bone mineral density. J Bone Miner Res. 2015;30(9):1717–25.
42. Li X, Ominsky MS, Warmington KS, et al. Increased bone formation and bone mass induced by sclerostin antibody is not affected by pretreatment or cotreatment with alendronate in osteopenic, ovariectomized rats. Endocrinology. 2011;152(9):3312–22.
43. Little DG, Peacock L, Mikulec K, et al. Combination sclerostin antibody and zoledronic acid treatment outperforms either treatment alone in a mouse model of osteogenesis imperfecta. Bone. 2017;101:96–103.
44. Ishizuka M, Tsuji S, Hirabayashi M, Kaneko K. Characteristic bands manifesting as

zebra lines on radiographs in osteogenesis imperfecta. Indian J Pediatr. 2017;84(4):336.
45. Cosman F, Crittenden DB, Adachi JD, et al. Romosozumab treatment in postmenopausal women with osteoporosis. N Engl J Med. 2016;375(16):1532–43.
46. Wen D, Qing L, Harrison G, Golub E, Akintoye SO. Anatomic site variability in rat skeletal uptake and desorption of fluorescently labeled bisphosphonate. Oral Dis. 2011;17(4):427–32.
47. Papakonstantinou O, Sakalidou M, Atsali E, Bizimi V, Mendrinou M, Alexopoulou E. Radiographic and MR imaging findings of the spine after bisphosphonate treatment, in a child with idiopathic juvenile osteoporosis. Case Rep Radiol. 2015;2015:727510.
48. Boyce AM, Tosi LL, Paul SM. Bisphosphonate treatment for children with disabling conditions. PM R. 2014;6(5):427–36.
49. Rauch F, Travers R, Plotkin H, Glorieux FH. The effects of intravenous pamidronate on the bone tissue of children and adolescents with osteogenesis imperfecta. J Clin Invest. 2002;110(9):1293–9.
50. Szalay EA. Bisphosphonate use in children with pediatric osteoporosis and other bone conditions. J Pediatr Rehabil Med. 2014;7(2):125–32.
51. Glorieux FH. Experience with bisphosphonates in osteogenesis imperfecta. Pediatrics. 2007;119 Suppl 2:S163–5.
52. Vesterby A, Mosekilde L, Gundersen HJG, et al. Biologically meaningful determinants of the in vitro strength of lumbar vertebrae. Bone. 1991;12(3):219–24.
53. Wegrzyn J, Roux J-P, Arlot ME, et al. Determinants of the mechanical behavior of human lumbar vertebrae after simulated mild fracture. J Bone Miner Res. 2011;26(4):739–46.
54. Ritzel H, Amling M, Pösl M, Hahn M, Delling G. The thickness of human vertebral cortical bone and its changes in aging and osteoporosis: a histomorphometric analysis of the complete spinal column from thirty-seven autopsy specimens. J Bone Miner Res. 1997;12(1):89–95.

Fig. **1.** Combination therapy to assess the effects after (*A*) a single cycle and (*B*) concurrent cycles of combination therapy. Region of interest placement in distal femoral

metaphysis to analyze the (*C*) short-term, (*D*) long-term, and (*E*) vertebral trabecular bone effects of combination therapy. (*F*) Proposed mechanism of action for combination therapy.

Fig. **2.** µCT analysis at the site of concurrent drug administration showed that PAM induced a significant dose-dependent increase in Tb.N whereas SclAb contributed to significant gains in both Tb.N and Tb.Th. Together these independent gains led to an additive gain in bone volume fraction with increasing PAM doses. Results of two-way ANOVA factors: *$p < 0.05$; **$p < 0.01$; ***$p < 0.001$; ****$p < 0.0001$.

Fig. **3.** (*A*) Entire metaphyseal trabecular bone ROI following two cycles of combination therapy showed that PAM continued to influence Tb.N while inducing no effects on Tb.Th. SclAb, however, induced gains in both Tb.Th and Tb.N. Each cyclic treatment was separately analyzed by subdividing the entire metaphyseal trabecular bone ROI into (*B*) cycle 1 and (*C*) cycle 2. Isolating the effects of each administered cycle confirmed that these low doses of PAM were weak in sustaining long-term trabeculae preservation. Results of two-way ANOVA factors: *$p < 0.05$; **$p < 0.01$; ***$p < 0.001$; ****$p < 0.0001$.

Fig. **4.** Histological sections of Brtl/+ metaphysis revealed short-term (*A*) and long-term (*B*) bone formation activity from a single and concurrent cycles of combination therapy, respectively. (*A*) At the BP-induced retention region, higher dosages of PAM were associated with greater primary trabeculae retention (yellow), while SclAb predominantly increased thickness (red). (*B*) Consecutive cycles of combination therapy showed a greater robust effect on bone mass with higher dosages of PAM. Calcein (green) was administered at the beginning and end of concurrent treatment cycles while alizarin (red) was administered prior to the second cyclic treatment. Sections visualized represent $n = 4$ per group.

Fig. **5.** (*A*) Microstructural properties of the vertebral trabecular bone reveal overall preservation of Tb.N with PAM and increased Tb.Th with SclAb after a single cycle of combination therapy. (*B*) With multiple treatment cycles, the response on Tb.N and Tb.Th was highly amplified leading to synergistic gains on bone mass. Results of two-way ANOVA factors: *$p < 0.05$; **$p < 0.01$; ***$p < 0.001$; ****$p < 0.0001$.

Fig. **6.** Histological coronal sections of Brtl/+ revealed bone formation activity from a

single (*A*) and multiple (*B*) cycles of combination therapy. (*A*) Under a single treatment cycle, higher dosages of PAM were associated to greater primary trabeculae retention (green), while SclAb predominantly increased thickness and connectivity between growth plates (red). (*B*) Multiple treatment cycles showed an evident trabecular retention response from both PAM and SclAb; however, SclAb also induced gains in trabecular thickness (green). Together a robust trabecular response was triggered leading to uniform trabecular bone distribution between growth plates. Sections visualized represent $n = 4$ per group.

Fig. **7.** (*A*) Femoral cortical analysis revealed SclAb influence on C.Th varies in the presence of PAM after a single treatment cycle. (*B*) Following subsequent cycles of combination therapy, C.Th nearly doubled solely in response to SclAb. (*C*) Functionally, multiple cycles PAM and SclAb led to additive gains in femoral stiffness and ultimate load with progressive PAM doses. Results of two-way ANOVA factors: $*p < 0.05$; $**p < 0.01$; $***p < 0.001$; $****p < 0.0001$.

Fig. **8.** (*A*) Vertebral cortical analysis revealed that after a single cycle, SclAb triggered greater gains in C.Th than when combined with PAM. (*B*) Following two cycles, however, consistent gains in C.Th were observed across all PAM dosages. (*C*) Functionally, following a single combination cycle, PAM effect on trabecular preservation helped improve vertebral stiffness while SclAb amplified these effects. Significant improvements in ultimate load were solely attributed to SclAb. (*D*) Both drugs improved ultimate load through an additive response, however, induced a synergistic effect on vertebral stiffness following multiple cycles of combination treatment. Results of two-way ANOVA factors: $*p < 0.05$; $**p < 0.01$; $***p < 0.001$; $****p < 0.0001$.

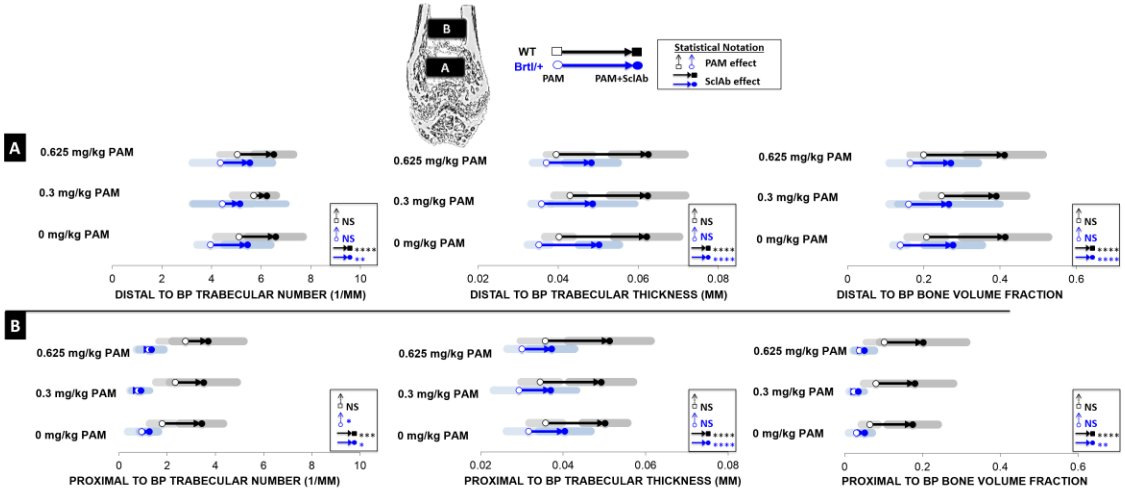

	Combination Treatment		Proximal to BP Band			Distal to BP Band		
			TbN (1/mm)	TbTh (mm)	BV/TV	TbN (1/mm)	TbTh (mm)	BV/TV
HET	0 mg/kg PAM	PBS	0.929 ± 0.556	0.032 ± 0.005	0.030 ± 0.020	3.954 ± 0.529	0.035 ± 0.003	0.139 ± 0.018
		SclAb	1.251 ± 0.384	0.040 ± 0.006	0.051 ± 0.019	5.447 ± 0.939	0.050 ± 0.005	0.277 ± 0.076
	0.3 mg/kg PAM	PBS	0.762 ± 0.305	0.029 ± 0.006	0.024 ± 0.012	4.428 ± 1.195	0.036 ± 0.003	0.160 ± 0.050
		SclAb	0.900 ± 0.380	0.037 ± 0.006	0.035 ± 0.017	5.142 ± 1.877	0.049 ± 0.011	0.266 ± 0.135
	0.625 mg/kg PAM	PBS	1.221 ± 0.495	0.030 ± 0.004	0.037 ± 0.016	4.355 ± 1.126	0.037 ± 0.003	0.164 ± 0.054
		SclAb	1.342 ± 0.512	0.037 ± 0.006	0.051 ± 0.025	5.542 ± 0.902	0.048 ± 0.007	0.271 ± 0.072
WT	0 mg/kg PAM	PBS	1.784 ± 0.508	0.036 ± 0.004	0.065 ± 0.021	5.108 ± 0.932	0.040 ± 0.004	0.207 ± 0.050
		SclAb	3.415 ± 0.913	0.050 ± 0.005	0.175 ± 0.065	6.577 ± 1.114	0.062 ± 0.008	0.413 ± 0.114
	0.3 mg/kg PAM	PBS	2.321 ± 0.776	0.034 ± 0.005	0.081 ± 0.032	5.700 ± 0.836	0.043 ± 0.004	0.247 ± 0.050
		SclAb	3.502 ± 1.389	0.049 ± 0.008	0.181 ± 0.099	6.223 ± 0.373	0.062 ± 0.009	0.390 ± 0.079
	0.625 mg/kg PAM	PBS	2.753 ± 1.112	0.036 ± 0.006	0.102 ± 0.047	5.038 ± 0.721	0.039 ± 0.003	0.200 ± 0.038
		SclAb	3.699 ± 1.479	0.051 ± 0.010	0.202 ± 0.112	6.504 ± 0.789	0.062 ± 0.009	0.412 ± 0.101

jbmr_3421_sm_Supporting Fig 1 .

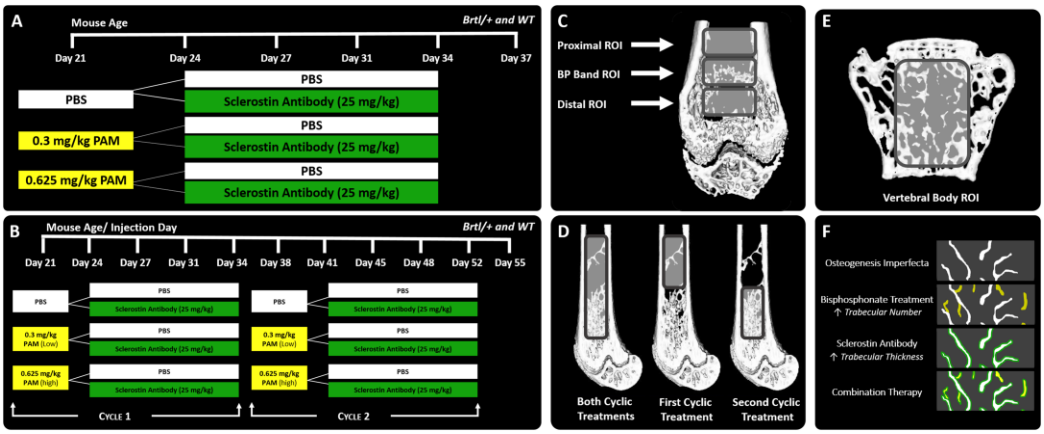

Figure 1

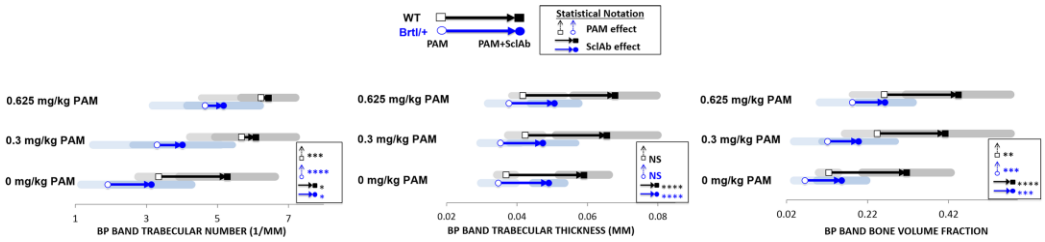

Figure 2

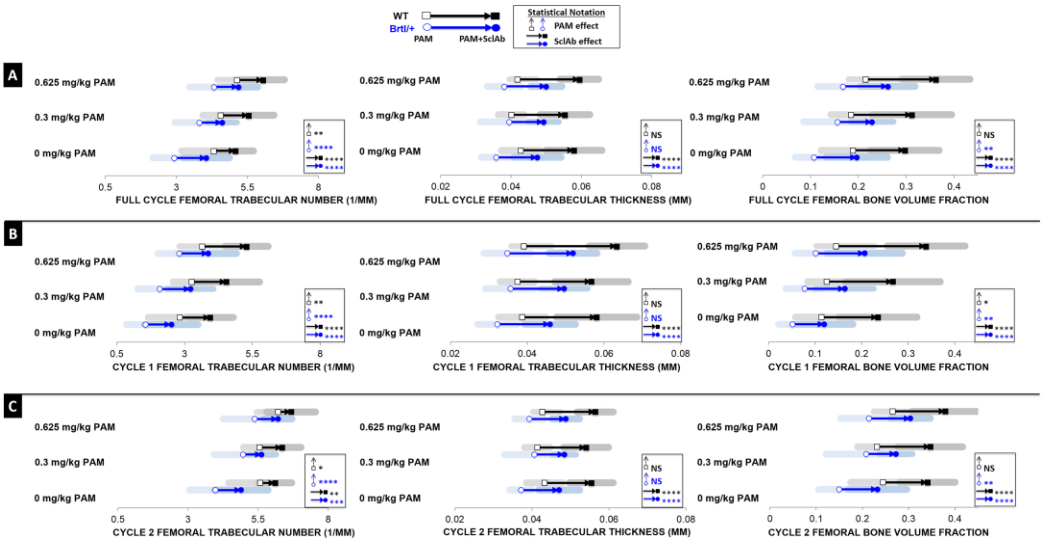

Figure 3

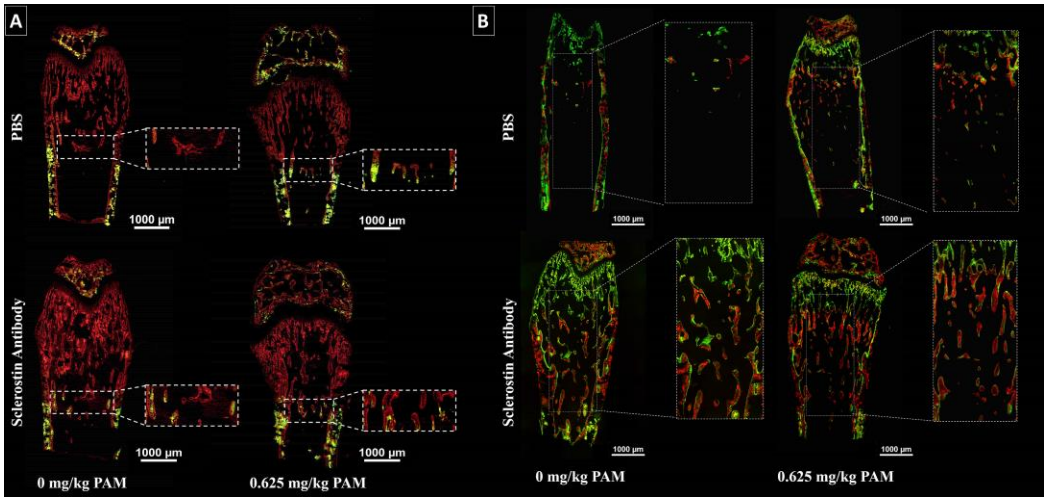

Figure 4

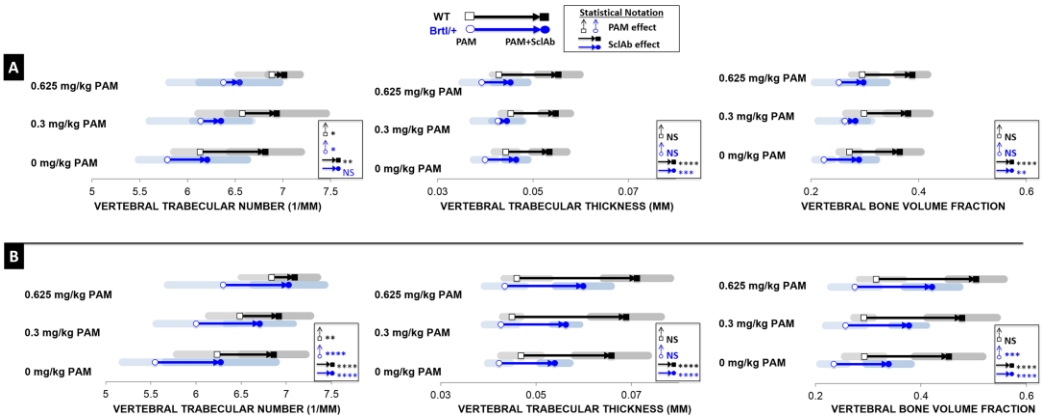

Figure 5

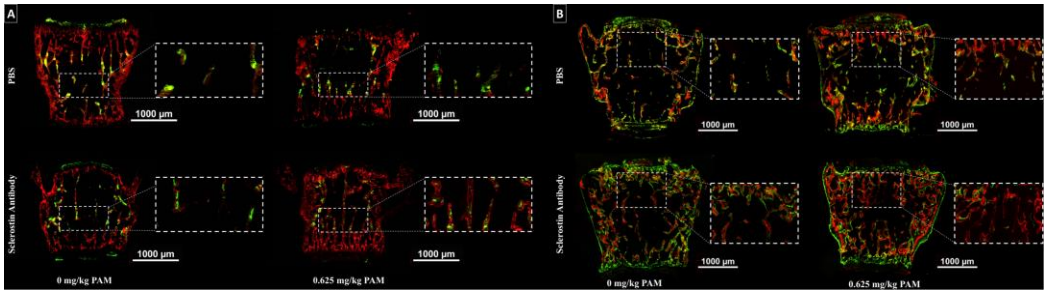

Figure 6

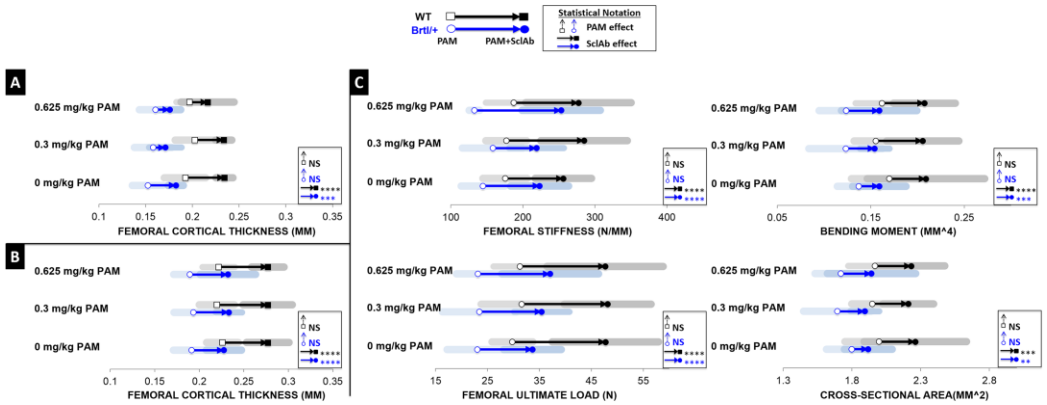

Figure 7

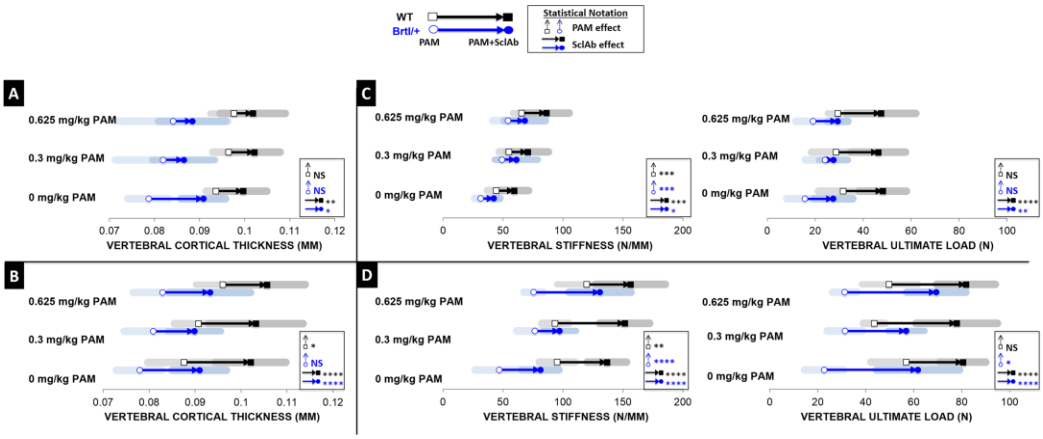

Figure 8